JPET Fast Forward. Published on July 2, 2021 as DOI: 10.1124/jpet.121.000491
This article has not been copyedited and formatted. The final version may differ from this version.

Small-molecule ISRIB reduces susceptibility to postinfarct atrial fibrillation in rats via the inhibition of integrated stress responses

Ting Zhang [1,2], Yong Wu [1], Zhengtao Hu [1], Wen Xing [1,3], Kun LV [3], Deguo Wang [1,3*], Nengwei Hu [1, 3, 4].

[1] Department of Gerontology, First Affiliated Hospital of Wannan Medical College, Wuhu, Anhui 241001.

[2] Department of Psychology, Wannan Medical College, Wuhu, Anhui 241001, China.

[3] Key Laboratory of Non-coding RNA Transformation Research of Anhui Higher Education Institution, The First Affiliated Hospital of Wannan Medical College, Wuhu, Anhui 241001, P.R. China.

[4] Department of Pharmacology & Therapeutics and Institute of Neuroscience, Trinity College, Dublin 2, Ireland.

JPET Fast Forward. Published on July 2, 2021 as DOI: 10.1124/jpet.121.000491
This article has not been copyedited and formatted. The final version may differ from this version.

Running Title Page.

Running title：ISRIB suppresses integrated stress responses and arrhythmia

Corresponding author：Deguo Wang

Address: 92nd Zheshan Western Road, Wuhu, Anhui 241001, P.R. China

Fax：0865535739107

&doctor1896

E-mail: wangdeguo@medmail.com.cn

Pages：36

Tables：2

Figures：8

References：60

Abstract：229

Introduction:366

Discussion:1114

Abbreviations

AF	atrial fibrillation
α-SMA	alpha smooth muscle actin
ATF4	activating transcription factor 4
Cav1.2	L-type voltage-dependent calcium channel 1.2
CHF	congestive heart failure
Cx43	connexin 43
ECG	Electrocardiogram
EDV	End-diastolic volume

JPET Fast Forward. Published on July 2, 2021 as DOI: 10.1124/jpet.121.000491
This article has not been copyedited and formatted. The final version may differ from this version.

EF	ejection fraction
eIF2α	eukaryotic translation initiation factor 2 α-subunit
ESV	End-diastolic volume
FS	fractional shortening
IL-1β	interleukin-1beta
iNOS	inducible nitric oxide synthase
ISR	integrated stress response
ISRIB	integrated stress response inhibitor
Kv4.3	voltage-activated A-type potassium ion channel 4.3
LA	left atrium
LAD	left anterior descending
LC3	light chain 3
LV	left ventricular
LVIDd	internal diameters of left ventricular at end-diastole
LVIDs	internal diameters of left ventricular at end-systole
LVPWd	left ventricular posterior wall thickness at end-diastole
LVPWs	left ventricular posterior wall thickness at end-systole
MI	myocardial infarction
Nav1.5	The voltage-gated sodium channel ***1.5***
TGFβ1	transforming growth factor beta1

Recommended section：Cardiovascular

JPET Fast Forward. Published on July 2, 2021 as DOI: 10.1124/jpet.121.000491
This article has not been copyedited and formatted. The final version may differ from this version.

Abstract

Phosphorylation of the eukaryotic translation initiation factor 2 α-subunit (eIF2α)，which subsequently upregulates activating transcription factor 4 (ATF4), is the core event in the integrated stress response (ISR) pathway. Previous studies indicate phosphorylation of eIF2α in atrial tissue in response to atrial fibrillation (AF). This study investigated the role of ISR pathway in experimental AF by using a small-molecule ISR inhibitor (ISRIB). Accordingly, rats were subjected to coronary artery occlusion to induce myocardial infarction (MI), or sham operation, and received either trans-ISRIB (2 mg/kg/day, i.p.) or vehicle for seven days. Thereafter, animals were subjected to the AF inducibility test by transesophageal rapid burst pacing followed by procurement of left atrium (LA) for assessment of atrial fibrosis, inflammatory indices, autophagy-related proteins, ISR activation, ion channel, and connexin43 expression. Results showed a significant increase in the AF vulnerability and the activation of ISR in LA as evidenced by enhanced eIF2α phosphorylation. ISRIB treatment suppressed upregulation of ATF4, fibrosis as indexed by determination of α-smooth muscle actin and collagen levels, inflammatory macrophage infiltration (i.e., CD68 and iNOS/CD68-positive macrophage) and autophagy as determined by expression of LC3. Further, ISRIB treatment reversed the expression of relevant ion channel (i.e., Nav1.5, Cav1.2, and Kv4.3) and Cx43 remodeling. Collectively, the results suggest that the ISR is a key pathway in pathogenesis of AF, post-MI, and represents a novel target for treatment of AF.

Keywords: atrial fibrillation, integrated stress response (ISR), autophagy, connexin43, fibrosis, macrophage, ISRIB

JPET Fast Forward. Published on July 2, 2021 as DOI: 10.1124/jpet.121.000491
This article has not been copyedited and formatted. The final version may differ from this version.

Significance Statement

The activation of integrated stress response (ISR) pathway as evidenced by enhanced eIF2α phosphorylation in left atrium plays a key role in atrial fibrillation (AF). A small-molecule ISR inhibitor (ISRIB) reduces AF occurrence and atrial arrhythmogenic substrate formation. The beneficial action of ISRIB may be mediated by suppressing ISR pathway-related cardiac fibrosis, inflammatory macrophage infiltration, autophagy, and restoring the expression of ion channel and Cx43. This study suggests a key dysfunctional role for ISR in pathogenesis of AF with implications for novel treatment.

JPET Fast Forward. Published on July 2, 2021 as DOI: 10.1124/jpet.121.000491
This article has not been copyedited and formatted. The final version may differ from this version.

1 Introduction

Atrial fibrillation (AF) is the most common sustained arrhythmia in clinical practice, and associated with stroke, congestive heart failure (CHF), and mortality(Guo et al., 2015; Lippi et al., 2020). With the aging of the population, AF has become a remarkable public health problem(Krijthe et al., 2013) associated with high costs of medical care of affected individuals (Stewart et al., 2002). Nowadays, available therapies for AF include Anti-arrhythmic drug, catheter ablation and surgical ablation, each with limitations like adverse effects, inconsistent efficacy and high recurrence rate(Heijman et al., 2016). Recent studies identified new pathophysiological mechanisms of AF including cardiac fibrosis(Nattel, 2017), oxidative stress(Antonopoulos et al., 2019), apoptosis, autophagy(Chen et al., 2011; Wiersma et al., 2017), inflammation(Zhou and Dudley, 2020) , and atrial ion-channel dysfunction, Ca^{2+}-handling abnormalities, autonomic neural dysregulation, and atrial remodeling (Andrade et al., 2014).

AF mechanism might be associated with the integrated stress response (ISR), which is always activated in chronic and persistent stress (Pakos-Zebrucka et al., 2016; Santos-Ribeiro et al., 2018). The ISR pathway is upregulated in atria of AF animal models indicating by enhanced phosphorylation of eukaryotic translation initiation factor 2α (eIF2α) and subsequently upregulation of activating transcription factor 4 (ATF4) (Pakos-Zebrucka et al., 2016). Previous studies have demonstrated eIF2α phosphorylation and ATF4 upregulation in the atria of experimental and human AF (Meyer-Roxlau et al., 2017; Wiersma et al., 2017; Freundt et al., 2018). ISR is also involved in atrial inflammation during chronic and persistent stress because it triggers artery inflammasome, interleukin-1beta secretion and

atherosclerosis (Onat et al., 2019).

A novel small-molecule ISR inhibitor (ISRIB) suppresses eIF2α cascade (Zyryanova et al., 2018; Kenner et al., 2019), and provides beneficial effects in neurodegenerative diseases(Sekine et al., 2015; Rabouw et al., 2019), atherosclerosis(Onat et al., 2019), and cancer (Mahameed et al., 2020). Rabouw et al. has demonstrated that ISRIB can mitigate undesirable outcomes of low-level ISR activation that may manifest neurological disease but leaves the cytoprotective effects of acute ISR activation intact (Rabouw et al., 2019). Therefore, we hypothesize that ISRIB may inhibit atrial fibrosis, inflammation, autophagy and dysfunction of ion channel, and AF susceptibility because chronic stress plays important role of in atrial remodeling and AF (Zhang et al., 2014; Wiersma et al., 2017).

2 Methods

2.1 Animals and drugs

Sixty male rats (Sprague Dawley, weight 200–250 g) were used for this study. All experimental procedures and protocols used in this study were approved by Animal Care and Use Ethics Committee of Yijishan Hospital (20180022) and performed in accordance with Guideline for the Care and Use of Laboratory Animals of the National Institutes of Health's guidelines principles. Thirty rats underwent left anterior descending (LAD) ligation to achieve myocardial infarction (MI), and the other 30 performed a sham operation without artery occlusion (Wu et al., 2020). After 24 h, both MI and sham control animals were randomly divided into subgroups that received trans-ISRIB (Sigma, SML0843, 2mg/kg/day in 0.5 ml saline, i.p.) or vehicle (0.5 ml saline, i.p.) for seven days. The dosage selection of trans-ISRIB

JPET Fast Forward. Published on July 2, 2021 as DOI: 10.1124/jpet.121.000491
This article has not been copyedited and formatted. The final version may differ from this version.

was based on our pre-test (supplementary data) and previous reports with minor modifications (Barragán-Iglesias et al., 2019; Onat et al., 2019). The high dose of ISRIB (5 mg/kg) led to reduced animal activity and body weight loss (supplementary Fig. S4) while low dose of ISRIB (0.25 mg/kg/day) did not inhibit myocardial inflammation (supplementary Fig. S3A and B) (Barragán-Iglesias et al., 2019; Onat et al., 2019). Thus, we used 2 mg/Kg/day of ISRIB for our studies. Seven days after administration of ISRIB or vehicle, all rats underwent echocardiographic and electrocardiographic studies.

2.2 Myocardial Infarction

MI was induced by coronary artery ligation at the site of the LAD as we have previously described (Wang et al., 2011; Zhu et al., 2015; Wang et al., 2017; Wu et al., 2020). The success of the MI protocol was judged by the ST-segment elevation on ECG (RM6240, Chengdu, China) and pallor transition in heart immediately after ligation. Rats in sham groups underwent the same procedures without LAD occlusion (Wu et al., 2020).

2.3 Ultrasound Cardiogram (UCG)

Seven days after MI, cardiac function was assessed blindly by a skilled echocardiologist (Zhu et al., 2015) using a HP SONOS 5500 (Philips Medical System, Ultrasound Inc., USA) which was equipped with a 21 MHz ultrasound transducer. Parasternal long-axis and short-axis views were acquired to measure the internal diameters of the left ventricles (LV) at end-diastole (LVIDd) and end-systole (LVIDs). The ejection fraction (EF) and the fractional shortening (FS) were calculated (Wang et al., 2011).

2.4 Electrocardiogram (ECG) and AF inducibility

The ECG trace was continuously recorded by a biological signal recording and analysis system (RM6240, Chengdu, China) which filtered out the signals below 10 Hz and above 100 Hz. The basic ECG was recorded consciously for 10 min for calculating ECG parameters such as P wave, QRS complex, PR interval, and QT intervals (Wang et al., 2011; Wu et al., 2020). The AF inducibility was performed by the transesophageal burst rapid pacing with a stimulating amplitude of 2-fold atrial capture threshold. Four consecutive bursts of rapid electrical stimulation for 30s (20, 30, 40, and 50 Hz) were applied to induce AF with 3 min pause (Cheng et al., 2019). AF was defined as an abnormal ECG showing rapid and fragmented P wave with absolute irregular RR intervals for at least 2 s (Cheng et al., 2019). The inducibility of AF was determined by the percentage of animals with induced AF. The duration of the longest episodes of AF was taken as inducible AF duration (Hohl et al., 2017).

2.5. Masson staining

Six left atrial (LA) tissue samples were dissected from every group and fixed in 4% paraformaldehyde, embedded in paraffin, and cut into sections (5 μm thick). Sections of LA were stained by Masson's staining to detect collagen as previously reported (Wang et al., 2016). The level of cardiac fibrosis was determined by the percentage of the fibrosis area to the total area (% cardiac fibrosis) using the ImageJ software (Media Cybernetics, Inc.) (Wu et al., 2020).

2.6. Immunohistochemistry and immunofluorescence labeling

Paraffin-embedded tissue sections of LA were processed and incubated with different primary antibodies (Supplementary Table 1) at 4 °C overnight (Wang et al., 2011). For

JPET Fast Forward. Published on July 2, 2021 as DOI: 10.1124/jpet.121.000491
This article has not been copyedited and formatted. The final version may differ from this version.

immunohistochemistry, six sections from every group were stained with the Envision system (Dako) and counterstained with hematoxylin. For immunofluorescence, secondary antibodies conjugated with fluorescein (FITC/CY3) were incubated for 1 h at room temperature. Then, 4,6-diamino-2-phenylindole (DAPI) was used to counterstain nuclei for further evaluation. The negative control staining was performed using the same protocol without adding any primary antibody. Images were recorded using a microscope (Nikon Eclipse C1, Tokyo, Japan) and quantified using the ImageJ software through calculating as the percentage of positively stained area to total area at high magnification (×400). For quantification of $CD68^+$ macrophages, the number of cells was counted in high magnification fields.

2.7. Western Blot

Protein expression was assayed using Western blot as described previously (Wang et al., 2019). In brief, six LA tissues, from each group, were processed and protein concentrations measured by the bicinchoninic acid assay. Equal amounts of proteins (50 μ g) were separated using 5% sodium dodecyl sulfate polyacrylamide gel electrophoresis (SDS-PAGE) and transferred onto a PVDF membrane. The membrane was then blocked with 5% non-fat dry milk in blocking buffer (10 mM Tris-HCl, 150 mM NaCl, and 0.2% Tween-20, pH 7.6) for 2 h at 37 °C and incubated with primary antibodies (Seen in supplementary Table 1) at certain dilutions at 4 °C overnight. The antibody binding was detected using a horseradish peroxidase (HRP)-conjugated secondary antibody (1:2000; Sigma) and visualized using an ECL kit for quantification for blots image (a Quantity-One software, Bio-Rad).

2.8. Statistical analysis

Values were expressed as means ± s.e.m. Significant differences between means were determined using the one-way ANOVA coupled with the Bonferroni *post hoc* test for multiple comparisons. The Mann–Whitney U test was used to test the difference of AF duration between the two MI groups. The Chi-square test was used to compare the inducibility of AF. A value of $P < 0.05$ was considered significant difference.

Results

3.1 ISRIB improves cardiac function in post-MI rats

Within the first 24 hours， 2 rats and 4 rats died in sham and MI group, respectively (13.3% vs 26.7%, P = 0.3894). From the second day, remaining rats received ISRIB or vehicle injection. On the second and third days, 2 rats died in MI group and one rat died in each other three groups (supplementary Fig. S1). No significant differences in animal survival rate were noted between sham and MI groups with or without ISRIB intervention (P =0.8571). On the seventh day, two rats in the Sham group one rat in the Sham+ ISRIB group died while under anesthesia and, thus, did not complete UCG and ECG assessment. (Supplementary Fig. S1). To assess whether ISRIB administration affects cardiac function post-MI, we investigated the echocardiographic parameters after ISRIB treatment in post-MI rats (Table 1). As shown in Table 1, rats in the MI group exhibited significantly reduced EF(%) and FS(%), expanded cardiac systolic volume and LVIDs compared with sham group. ISRIB treatment significantly ameliorated the decline of EF, FS, and ventricular enlargement in MI rats but the treatment did not affect the aforementioned parameters in sham-operated animals.

3.2 ISRIB inhibits AF inducibility in post-MI rats

JPET Fast Forward. Published on July 2, 2021 as DOI: 10.1124/jpet.121.000491
This article has not been copyedited and formatted. The final version may differ from this version.

To determine whether ISRIB may be beneficial in AF, we tested the AF inducibility and ECG parameters in post-MI rats. Figure 1A shows that atrial burst rapid pacing could induce AF. Compared with the sham group, the MI group exhibited significantly vulnerability to AF (81.82% vs 0%, $P < 0.05$). ISRIB significantly reduced the AF inducibility in MI rats (33.3% vs 81.82%, $P < 0.05$) (Fig. 1B). The longest AF duration was not different between the two MI groups (Fig. 1C). We also observed increases in P wave duration, QRS wave complexes, PR interval and QT interval compared with the sham group ($P < 0.01$). ISRIB significantly reduced these changes in MI rats ($P < 0.01$, Table 2).

3.3 ISRIB prevents atrial fibrosis in the LA in post-MI rats

Figure 2A shows representative illustrations for atrial fibrosis. ISRIB treatment significantly reduced fibrotic areas of the LA in MI rats but not in normal rats (Fig. 2D). As shown in Figure 2B, the expression levels of the alpha-smooth muscle actin (α-SMA, a marker for the proliferation of myofibroblasts) in MI rats were significantly higher than those in normal rats. ISRIB significantly ameliorated the α-SMA expression in LA from the MI group but not from the normal group (Fig. 2E). As shown in Figure 3C, a remarkable deposition of collagen I in the LA of the MI group was observed compared with that of the sham group. ISRIB treatment significantly reduced collagen I productions in MI rats but not in normal rats (Fig. 2F). These results indicated that ISR had a role in atrial fibrosis by promoting myofibroblast transition and collagen deposition after MI.

3.4 ISRIB restores ATF4 expression without affecting p-eIF2α in the LA in post-MI rats

ISR activation leads to global reduction in protein synthesis but preferentially enhances

JPET Fast Forward. Published on July 2, 2021 as DOI: 10.1124/jpet.121.000491
This article has not been copyedited and formatted. The final version may differ from this version.

translation of some mRNAs such as ATF4. Using fluorescent immunostaining, we found that the level of ATF4 remarkably increased in LA from MI group compared with sham group (Fig. 3A and B). ISRIB treatment significantly reversed ATF4 level in post-MI rats (Fig. 3A and B). Western blot further confirmed that ISRIB treatment significantly inhibited the ATF4 protein expression in the LA from MI rats but not from normal rats (Fig. 3C and E). The key regulation step in the ISR is the phosphorylation of eIF2α. We found that ISRIB treatment did not alter the expression levels of eIF2α and p-eIF2α in both sham and MI rats (Fig. 3C and D). These results indicate that ISRIB restores ATF4 protein expression in the nuclei of myocytes from LA through suppressing the downstream of the eIF2α pathway.

3.5 ISRIB regulates atrial macrophage infiltration in post-MI rats

Previous studies have reported inflammatory response and macrophage infiltration in atrial tissue including M1 ($iNOS^+/CD68^+$) and M2 subtypes ($CD163^+/CD68^+$) (Sun et al., 2016; Liu et al., 2019). As shown in Figures 4A and C, a remarkable increase of total CD68+ macrophages was observed in LA from MI rats, which could be reduced by ISRIB treatment. Moreover, the distributions of iNOS-positive and CD163-positive immunofluorescence signals are not limited to macrophages and increase significantly in atrial tissue from MI rats (Fig. 4A and B). ISRIB treatment reduced $iNOS^+/CD68^+$ cells (Fig. 4D) without changing $CD163^+/CD68^+$ cells (Fig. 4E). These results indicate that ISR may play an important role in macrophages infiltration into atrial tissue from post-MI rats.

3.6 ISRIB modulates the expression of autophagy-related protein in the LA in post-MI rats

JPET Fast Forward. Published on July 2, 2021 as DOI: 10.1124/jpet.121.000491
This article has not been copyedited and formatted. The final version may differ from this version.

We also determined the expression of autophagy markers, LC3, which is activated and incorporated into autophagosomes(Wiersma et al., 2017; Yuan et al., 2018). Using fluorescent immunostaining, we found a significant increase in the expression of the autophagy marker LC3 in LA in MI rats which was completely reversed by ISRIB (Fig. 5A and C). Western blot analysis also confirmed an increase of LC3-II and LC3-II/LC3-I ratio in LA, and ISRIB treatment significantly reduced the upregulation of LC3 in MI rats (Fig. 5B and D). These results suggest a biologically contribution of ISR to endoplasmic reticulum stress and autophagy.

3.7 ISRIB stabilizes the connexin43 (Cx43) expression in the LA in post-MI rats

To determine whether the reduction in ISR activation affects the Cx43 expression and distribution in atria, we tested the Cx43 level using fluorescent immunostaining. The Cx43 was distributed in the intercalated disk (end of myocardial cell) in the sham-operated group but redistributed to the lateral cell membrane in the MI group (supplementary Fig. S2A and B). As shown in Figure 6A, Cx43 immunostaining was markedly reduced in LA in MI rats. Accordingly, the relative value of the Cx43-positive area decreased significantly in the MI group which was reversed by ISRIB treatment (Fig. 6B). These results suggest that the ISR activation may be associated with the gap junction remodeling.

3.8 ISRIB keeps ion channel expression in the LA in post-MI rat

The abnormal ion channel is closely related to the action potentials of atrial myocytes, which facilitates atrial re-entry via the atrial heterogeneous conduction and focal trigger activity (Nattel et al., 2007). The protein expression of some ion channel-related proteins

JPET Fast Forward. Published on July 2, 2021 as DOI: 10.1124/jpet.121.000491
This article has not been copyedited and formatted. The final version may differ from this version.

(such as Nav1.5, L-type calcium channel α1c [Cav1.2], and Kv4.3), which are involved in AF, were assessed to learn the role of ISR in the generation of AF (Nattel et al., 2007). We found significant reduction in protein expression for Nav1.5 (Fig. 7A and B), Cav1.2 (Fig. 7A and C), and Kv4.3 (Fig. 7A and C) in LA in MI rats (Fig 7). Moreover, ISRIB treatment significantly restored the protein expression levels of all three ion channels (Fig. 7). These results support the notion that ISR results in the down regulation of the protein expression of the above ion channels in LA.

4. Discussion

This study demonstrates that ISR activation in the LA is associated with post-MI AF. We have also observed that MI promoted atrial fibrosis, inflammation, autophagy, and downregulated protein expression level of Cx43 and ion-channel subunits including Nav1.5, Cav1.2 and Kv4.3. A small-molecule ISR inhibitor called ISRIB (trans-ISRIB) ameliorated LV dysfunction and AF inducibility accompanied with reduced atrial inflammation, fibrosis, and autophagy as well as reversal of protein expression of ion channels and Cx43 in the LA post-MI.

We observed that ISRIB restored aberrant high ATF4 protein expression in the LA from MI rats without changing total eIF2α and p-eIF2α. As the core event in the ISR pathway, the phosphorylation of eIF2α leads to the upregulation of ATF4 and the prohibition of global protein synthesis (Pakos-Zebrucka et al., 2016). ISRIB enhances long-term memory and ameliorates neurodegenerative diseases (Sekine et al., 2015; Sidrauski et al., 2015; Chou et al., 2017; Tsai et al., 2018). It mitigates low-level ISR activation and keeps acute ISR activation

JPET Fast Forward. Published on July 2, 2021 as DOI: 10.1124/jpet.121.000491
This article has not been copyedited and formatted. The final version may differ from this version.

intact, which is helpful for neurological diseases (Rabouw et al., 2019). Thus, ISRIB may protect against chronic ISR-related diseases such as atherosclerosis(Onat et al., 2019) and type 2 diabetes mellitus(Pandey et al., 2019). Recent studies indicate the involvement of endoplasmic reticulum stress which appeared as upregulation of eIF2α and ATF4, in atria of experimental and human AF (Wiersma et al., 2017; Freundt et al., 2018). Therefore, ISRIB may inhibit AF by suppressing ISR in atria. Indeed, the present study showed that ISRIB significantly reduced the AF inducibility to rapid atrial stimulation. We deduce that ISR may be involved in the atrial proarrhythmic substrates of AF in post-MI rats.

The atrial fibrosis is associated with low-conduction velocity and long activation time(Krul et al., 2015). Suppression of atrial fibrosis prevent AF through “upstream therapy”, including renin–angiotensin–aldosterone system, inflammatory mediators, and other signaling targets(Li et al., 2001; Nattel et al., 2020). Under stress conditions, the transforming growth factor beta1 (TGFβ1) promotes fibroblasts to proliferate and differentiate into profibrotic collagen-secreting myofibroblasts, leading to atrial collagen deposition, extracellular matrix remodeling, and fibrosis(Nattel et al., 2020). In the present study, we observed that the ISRIB reduced more than 50% of the fibrotic areas and inhibited the collagen type I deposition and α-SMA expression in the LA from MI rats thereby suggesting that ISR is involved in atrial fibrosis.

The atrial inflammation mediates electrical and structural remodeling, and modulates calcium homeostasis and gap junction (Hu et al., 2015; Packer, 2020). Patients with AF have an increased immune cell infiltration in the atria, such as $CD45^+$ lymphocytes, $CD68^+$ macrophages (Chen et al., 2008), $CD163^+$ macrophages(Watson et al., 2020), and

JPET Fast Forward. Published on July 2, 2021 as DOI: 10.1124/jpet.121.000491
This article has not been copyedited and formatted. The final version may differ from this version.

proinflammatory cytokines(Zhou and Dudley, 2020). The suppression of atrial inflammation has antiarrhythmic effects against AF in the early phase of MI(Deftereos et al., 2012; Lakin et al., 2019; Liu et al., 2019; Zhou and Dudley, 2020). In this study, ISRIB reduces total $CD68^+$ macrophage infiltration in LA, suggesting involvement of ISR in atrial inflammation. We also observed that some infiltrated $CD68^+$ macrophages in LA from MI rats were iNOS-positive but CD163-negative. ISRIB treatment reduced the level of iNOS but not CD163 in atria. CD163-positive macrophages have been known as a marker of M2 subtype(Liu et al., 2019), also have potential pro-fibrotic role in atrium from AF (Watson et al., 2020). Thus, the ISR plays an important role in regulating atrial proinflammatory response. Further study is needed to clarify the detailed mechanism of ISR in atrial inflammation and the occurrence of AF.

Previous studies have showed that the autophagy-related protein LC3 increased in the left atrium of human chronic AF (Shingu et al., 2020) and AF animals (Wiersma et al., 2017; Yuan et al., 2018). Our results showed that MI promoted LC3 expression in LA which was partly reversed by ISRIB treatment. Autophagy may be an important mechanism of AF (Kroemer et al., 2010) because previous studies have confirmed that autophagy could induce atrial electrical remodeling including L-type Ca^{2+}-current reduction and selective degradation of Cav1.2(Wiersma et al., 2017; Yuan et al., 2018). Autophagy also leads to eIF2α phosphorylation and ATF4 upregulation in experimental and human AF(Wiersma et al., 2017). Thus, ISR activation might be associated with autophagy and play an important role of AF post-MI.

Several ion channels and gap junction are involved in electrical remodeling promoting AF (Nattel et al., 2007; Nattel et al., 2020) and facilitates atrial re-entry and focal trigger

JPET Fast Forward. Published on July 2, 2021 as DOI: 10.1124/jpet.121.000491
This article has not been copyedited and formatted. The final version may differ from this version.

activity(Nattel et al., 2007). Reduction of the Nav1.5 expression contributes to AF by delaying conduction and promoting reentry(Martin et al., 2019; McCauley et al., 2020). The protein and gene expression levels of voltage-dependent K^+ channel 4.3 (Kv4.3) are downregulated in atria from AF patients and models (Brundel et al., 2001a; Brundel et al., 2001b; Bosch et al., 2003).The protein and gene expression of Cav1.2 decreased in LA in models of atrial tachycardia (Nakatani et al., 2013; Martins et al., 2014; Chong et al., 2015). In the present study, we found that ISRIB ameliorates the reduction in the protein expression levels of Nav1.5, Cav1.2, and Kv4.2 in LA from post-MI. We also found that ISRIB improves the Cx43 expression and distribution. Cx43 is a major component of gap junction between myocytes and its abnormality may cause atrial spatial heterogeneity of conduction(Nattel et al., 2007). In a rat model of spontaneous hypertension, the AF vulnerability is associated with slow conduction velocity and low Cx43 expression, phosphorylation and redistribution(Parikh et al., 2013). Thus, our results suggest that ISRIB may attenuate the atrial electrical remodeling by preventing the downregulation of functional transmembrane proteins including ion channel and Cx43 in LA.

As key mechanisms of initial and maintenance of AF, ion channels and gap junction may be altered by ischemia through atrial fibrosis(Nattel, 2017), inflammation(Zhou and Dudley, 2020), and autophagy in LA (Wiersma et al., 2017; Packer, 2020). In the present study, ISRIB inhibited atrial fibrosis, inflammation and autophagy in LA. Therefore, ISR-pathway might contribute to the proarrhythmic mechanism of AF. Overall, ISRIB blocks the ATF4 protein expression without affecting p-eIF2α in LA post-MI, which results in the restoration of normal functional protein synthesis (including ion channels and gap junction) by suppressing

JPET Fast Forward. Published on July 2, 2021 as DOI: 10.1124/jpet.121.000491
This article has not been copyedited and formatted. The final version may differ from this version.

the downstream of the eIF2α pathway.

This study has several limitations. First, we did not determine spontaneous AF in non-anesthesia rats due to lack of relevant physiological monitoring system for small animal. Second, we did not evaluate the electrophysiological functions of ion channel (Na^+, K^+, and Ca^{2+}) from atrial myocytes although we have determined the protein expression of Nav1.5, Cav1.2, and Kv4.2. Third, other signaling pathways relevant to ISR may also play roles in AF. Fourth, further studies are needed to establish the long-term therapeutic effects of ISRIB on AF in the context of assessment of its potential toxic effects.

Conclusions

Despite the existence of several limitations, this study has revealed that the trans-ISRIB could suppress ISR in ischemia atria which are at risk for AF. The possible mechanisms may be related to cardiac fibrosis, inflammatory cell infiltration, autophagy-related protein LC3 expression, and the remodeling of ion channel and Cx43. Considering the limitations of current therapies for AF, this study suggests that the ISR is a key pathway in pathogenesis of AF, and represents a novel target for treatment of AF.

Acknowledgements

We thank Professor He Yang for valuable assistance in writing this manuscript.

Authorship Contributions

Participated in research design: Deguo Wang and Kun Lv.

Conducted experiments: Zhengtao Hu, Ting Zhang and Yong Wu.

Provision of analytical tools: Ting Zhang.

Performed data analysis: Deguo Wang and Wen Xing.

Wrote or contributed to the writing of the manuscript: Nengwei Hu and Deguo Wang.

Competing financial interests

We have no conflict of interest to disclose.

The data used to support the findings of this study are included within the article and supplementary materials.

References

Andrade J, Khairy P, Dobrev D and Nattel S (2014) The clinical profile and pathophysiology of atrial fibrillation: relationships among clinical features, epidemiology, and mechanisms. *Circulation research* **114**:1453-1468.

Antonopoulos AS, Goliopoulou A, Oikonomou E, Tsalamandris S, Papamikroulis GA, Lazaros G, Tsiamis E, Latsios G, Brili S, Papaioannou S, Gennimata V and Tousoulis D (2019) Redox State in Atrial Fibrillation Pathogenesis and Relevant Therapeutic Approaches. *Current medicinal chemistry* **26**:765-779.

Barragán-Iglesias P, Kuhn J, Vidal-Cantú GC, Salinas-Abarca AB, Granados-Soto V, Dussor GO, Campbell ZT and Price TJ (2019) Activation of the integrated stress response in nociceptors drives methylglyoxal-induced pain. *Pain* **160**:160-171.

Bosch RF, Scherer CR, Rüb N, Wöhrl S, Steinmeyer K, Haase H, Busch AE, Seipel L and Kühlkamp V (2003) Molecular mechanisms of early electrical remodeling: transcriptional downregulation of ion channel subunits reduces I(Ca,L) and I(to) in rapid atrial pacing in rabbits. *Journal of the American College of Cardiology* **41**:858-869.

Brundel BJ, Van Gelder IC, Henning RH, Tieleman RG, Tuinenburg AE, Wietses M, Grandjean JG, Van Gilst WH and Crijns HJ (2001a) Ion channel remodeling is related to intraoperative atrial effective refractory periods in patients with paroxysmal and persistent atrial fibrillation. *Circulation* **103**:684-690.

Brundel BJ, Van Gelder IC, Henning RH, Tuinenburg AE, Wietses M, Grandjean JG, Wilde AA, Van Gilst WH and Crijns HJ (2001b) Alterations in potassium channel gene expression

in atria of patients with persistent and paroxysmal atrial fibrillation: differential regulation of protein and mRNA levels for K+ channels. *Journal of the American College of Cardiology* **37**:926-932.

Chen MC, Chang JP, Liu WH, Yang CH, Chen YL, Tsai TH, Wang YH and Pan KL (2008) Increased inflammatory cell infiltration in the atrial myocardium of patients with atrial fibrillation. *The American journal of cardiology* **102**:861-865.

Chen MC, Chang JP, Wang YH, Liu WH, Ho WC and Chang HW (2011) Autophagy as a mechanism for myolysis of cardiomyocytes in mitral regurgitation. *European journal of clinical investigation* **41**:299-307.

Cheng C, Liu H, Tan C, Tong D, Zhao Y, Liu X, Si W, Wang L, Liang L, Li J, Wang C, Chen Q, Du Y, Wang QK and Ren X (2019) Mutation in NPPA causes atrial fibrillation by activating inflammation and cardiac fibrosis in a knock-in rat model. *FASEB journal : official publication of the Federation of American Societies for Experimental Biology* **33**:8878-8891.

Chong E, Chang SL, Hsiao YW, Singhal R, Liu SH, Leha T, Lin WY, Hsu CP, Chen YC, Chen YJ, Wu TJ, Higa S and Chen SA (2015) Resveratrol, a red wine antioxidant, reduces atrial fibrillation susceptibility in the failing heart by PI3K/AKT/eNOS signaling pathway activation. *Heart rhythm* **12**:1046-1056.

Chou A, Krukowski K, Jopson T, Zhu PJ, Costa-Mattioli M, Walter P and Rosi S (2017) Inhibition of the integrated stress response reverses cognitive deficits after traumatic brain injury. *Proceedings of the National Academy of Sciences of the United States of America* **114**:E6420-E6426.

Deftereos S, Giannopoulos G, Kossyvakis C, Efremidis M, Panagopoulou V, Kaoukis A, Raisakis K, Bouras G, Angelidis C, Theodorakis A, Driva M, Doudoumis K, Pyrgakis V and Stefanadis C (2012) Colchicine for prevention of early atrial fibrillation recurrence after pulmonary vein isolation: a randomized controlled study. *Journal of the American College of Cardiology* **60**:1790-1796.

Freundt JK, Frommeyer G, Wotzel F, Huge A, Hoffmeier A, Martens S, Eckardt L and Lange PS (2018) The Transcription Factor ATF4 Promotes Expression of Cell Stress Genes and Cardiomyocyte Death in a Cellular Model of Atrial Fibrillation. *BioMed research international* **2018**:3694362.

Garaeva AA, Kovaleva IE, Chumakov PM and Evstafieva AG (2016) Mitochondrial dysfunction induces SESN2 gene expression through Activating Transcription Factor 4. *Cell cycle* **15**:64-71.

Guo Y, Tian Y, Wang H, Si Q, Wang Y and Lip GYH (2015) Prevalence, incidence, and lifetime risk of atrial fibrillation in China: new insights into the global burden of atrial fibrillation. *Chest* **147**:109-119.

Heijman J, Algalarrondo V, Voigt N, Melka J, Wehrens XH, Dobrev D and Nattel S (2016) The value of basic research insights into atrial fibrillation mechanisms as a guide to therapeutic innovation: a critical analysis. *Cardiovascular research* **109**:467-479.

Hohl M, Lau DH, Müller A, Elliott AD, Linz B, Mahajan R, Hendriks JML, Böhm M, Schotten U, Sanders P and Linz D (2017) Concomitant Obesity and Metabolic Syndrome Add to the Atrial Arrhythmogenic Phenotype in Male Hypertensive Rats. *Journal of the American Heart Association* **6**.

Hu YF, Chen YJ, Lin YJ and Chen SA (2015) Inflammation and the pathogenesis of atrial fibrillation. *Nature reviews Cardiology* **12**:230-243.

Kenner LR, Anand AA, Nguyen HC, Myasnikov AG, Klose CJ, McGeever LA, Tsai JC, Miller-Vedam LE, Walter P and Frost A (2019) eIF2B-catalyzed nucleotide exchange and phosphoregulation by the integrated stress response. *Science* **364**:491-495.

Krijthe BP, Kunst A, Benjamin EJ, Lip GY, Franco OH, Hofman A, Witteman JC, Stricker BH and Heeringa J (2013) Projections on the number of individuals with atrial fibrillation in the European Union, from 2000 to 2060. *European heart journal* **34**:2746-2751.

Kroemer G, Marino G and Levine B (2010) Autophagy and the integrated stress response. *Molecular cell* **40**:280-293.

Krul SP, Berger WR, Smit NW, van Amersfoorth SC, Driessen AH, van Boven WJ, Fiolet JW, van Ginneken AC, van der Wal AC, de Bakker JM, Coronel R and de Groot JR (2015) Atrial fibrosis and conduction slowing in the left atrial appendage of patients undergoing thoracoscopic surgical pulmonary vein isolation for atrial fibrillation. *Circulation Arrhythmia and electrophysiology* **8**:288-295.

Lakin R, Polidovitch N, Yang S, Guzman C, Gao X, Wauchop M, Burns J, Izaddoustdar F and Backx PH (2019) Inhibition of soluble TNFalpha prevents adverse atrial remodeling and atrial arrhythmia susceptibility induced in mice by endurance exercise. *Journal of molecular and cellular cardiology* **129**:165-173.

Li D, Shinagawa K, Pang L, Leung TK, Cardin S, Wang Z and Nattel S (2001) Effects of angiotensin-converting enzyme inhibition on the development of the atrial fibrillation substrate in dogs with ventricular tachypacing-induced congestive heart

failure. *Circulation* **104**:2608-2614.

Lippi G, Sanchis-Gomar F and Cervellin G (2020) Global epidemiology of atrial fibrillation: An increasing epidemic and public health challenge. *International journal of stroke : official journal of the International Stroke Society*:1747493019897870.

Liu M, Li W, Wang H, Yin L, Ye B, Tang Y and Huang C (2019) CTRP9 Ameliorates Atrial Inflammation, Fibrosis, and Vulnerability to Atrial Fibrillation in Post-Myocardial Infarction Rats. *Journal of the American Heart Association* **8**:e013133.

Mahameed M, Boukeileh S, Obiedat A, Darawshi O, Dipta P, Rimon A, McLennan G, Fassler R, Reichmann D, Karni R, Preisinger C, Wilhelm T, Huber M and Tirosh B (2020) Pharmacological induction of selective endoplasmic reticulum retention as a strategy for cancer therapy. *Nature communications* **11**:1304.

Martin B, Gabris B, Barakat AF, Henry BL, Giannini M, Reddy RP, Wang X, Romero G and Salama G (2019) Relaxin reverses maladaptive remodeling of the aged heart through Wnt-signaling. *Scientific reports* **9**:18545.

Martins RP, Kaur K, Hwang E, Ramirez RJ, Willis BC, Filgueiras-Rama D, Ennis SR, Takemoto Y, Ponce-Balbuena D, Zarzoso M, O'Connell RP, Musa H, Guerrero-Serna G, Avula UM, Swartz MF, Bhushal S, Deo M, Pandit SV, Berenfeld O and Jalife J (2014) Dominant frequency increase rate predicts transition from paroxysmal to long-term persistent atrial fibrillation. *Circulation* **129**:1472-1482.

McCauley MD, Hong L, Sridhar A, Menon A, Perike S, Zhang M, da Silva IB, Yan J, Bonini MG, Ai X, Rehman J and Darbar D (2020) Ion Channel and Structural Remodeling in Obesity: Mediated Atrial Fibrillation. *Circulation Arrhythmia and electrophysiology*.

Meyer-Roxlau S, Lämmle S, Opitz A, Künzel S, Joos JP, Neef S, Sekeres K, Sossalla S, Schöndube F, Alexiou K, Maier LS, Dobrev D, Guan K, Weber S and El-Armouche A (2017) Differential regulation of protein phosphatase 1 (PP1) isoforms in human heart failure and atrial fibrillation. *Basic research in cardiology* **112**:43.

Nakatani Y, Nishida K, Sakabe M, Kataoka N, Sakamoto T, Yamaguchi Y, Iwamoto J, Mizumaki K, Fujiki A and Inoue H (2013) Tranilast prevents atrial remodeling and development of atrial fibrillation in a canine model of atrial tachycardia and left ventricular dysfunction. *Journal of the American College of Cardiology* **61**:582-588.

Nattel S (2017) Molecular and Cellular Mechanisms of Atrial Fibrosis in Atrial Fibrillation. *JACC Clinical electrophysiology* **3**:425-435.

Nattel S, Heijman J, Zhou L and Dobrev D (2020) Molecular Basis of Atrial Fibrillation Pathophysiology and Therapy: A Translational Perspective. *Circulation research* **127**:51-72.

Nattel S, Maguy A, Le Bouter S and Yeh YH (2007) Arrhythmogenic ion-channel remodeling in the heart: heart failure, myocardial infarction, and atrial fibrillation. *Physiological reviews* **87**:425-456.

Onat UI, Yildirim AD, Tufanli O, Cimen I, Kocaturk B, Veli Z, Hamid SM, Shimada K, Chen S, Sin J, Shah PK, Gottlieb RA, Arditi M and Erbay E (2019) Intercepting the Lipid-Induced Integrated Stress Response Reduces Atherosclerosis. *Journal of the American College of Cardiology* **73**:1149-1169.

Packer M (2020) Characterization, Pathogenesis, and Clinical Implications of Inflammation-Related Atrial Myopathy as an Important Cause of Atrial Fibrillation. *Journal of the*

American Heart Association **9**:e015343.

Pakos-Zebrucka K, Koryga I, Mnich K, Ljujic M, Samali A and Gorman AM (2016) The integrated stress response. *EMBO reports* **17**:1374-1395.

Pandey VK, Mathur A, Khan MF and Kakkar P (2019) Activation of PERK-eIF2alpha-ATF4 pathway contributes to diabetic hepatotoxicity: Attenuation of ER stress by Morin. *Cellular signalling* **59**:41-52.

Parikh A, Patel D, McTiernan CF, Xiang W, Haney J, Yang L, Lin B, Kaplan AD, Bett GC, Rasmusson RL, Shroff SG, Schwartzman D and Salama G (2013) Relaxin suppresses atrial fibrillation by reversing fibrosis and myocyte hypertrophy and increasing conduction velocity and sodium current in spontaneously hypertensive rat hearts. *Circulation research* **113**:313-321.

Rabouw HH, Langereis MA, Anand AA, Visser LJ, de Groot RJ, Walter P and van Kuppeveld FJM (2019) Small molecule ISRIB suppresses the integrated stress response within a defined window of activation. *Proceedings of the National Academy of Sciences of the United States of America* **116**:2097-2102.

Santos-Ribeiro D, Godinas L, Pilette C and Perros F (2018) The integrated stress response system in cardiovascular disease. *Drug discovery today* **23**:920-929.

Sekine Y, Zyryanova A, Crespillo-Casado A, Fischer PM, Harding HP and Ron D (2015) Stress responses. Mutations in a translation initiation factor identify the target of a memory-enhancing compound. *Science* **348**:1027-1030.

Shingu Y, Takada S, Yokota T, Shirakawa R, Yamada A, Ooka T, Katoh H, Kubota S and Matsui Y (2020) Correlation between increased atrial expression of genes related to fatty acid

metabolism and autophagy in patients with chronic atrial fibrillation. *PloS one* **15**:e0224713.

Sidrauski C, McGeachy AM, Ingolia NT and Walter P (2015) The small molecule ISRIB reverses the effects of eIF2alpha phosphorylation on translation and stress granule assembly. *eLife* **4**.

Stewart S, Hart CL, Hole DJ and McMurray JJ (2002) A population-based study of the long-term risks associated with atrial fibrillation: 20-year follow-up of the Renfrew/Paisley study. *The American journal of medicine* **113**:359-364.

Sun Z, Zhou D, Xie X, Wang S, Wang Z, Zhao W, Xu H and Zheng L (2016) Cross-talk between macrophages and atrial myocytes in atrial fibrillation. *Basic research in cardiology* **111**:63.

Tsai JC, Miller-Vedam LE, Anand AA, Jaishankar P, Nguyen HC, Renslo AR, Frost A and Walter P (2018) Structure of the nucleotide exchange factor eIF2B reveals mechanism of memory-enhancing molecule. *Science* **359**.

Wang D, Wu Y, Chen Y, Wang A, Lv K, Kong X, He Y and Hu N (2019) Focal selective chemo-ablation of spinal cardiac afferent nerve by resiniferatoxin protects the heart from pressure overload-induced hypertrophy. *Biomedicine & pharmacotherapy = Biomedecine & pharmacotherapie* **109**:377-385.

Wang D, Zhang F, Shen W, Chen M, Yang B, Zhang Y and Cao K (2011) Mesenchymal stem cell injection ameliorates the inducibility of ventricular arrhythmias after myocardial infarction in rats. *International journal of cardiology* **152**:314-320.

Wang D, Zhu H, Yang Q and Sun Y (2016) Effects of relaxin on cardiac fibrosis, apoptosis, and

tachyarrhythmia in rats with myocardial infarction. *Biomedicine & pharmacotherapy = Biomedecine & pharmacotherapie* **84**:348-355.

Wang HJ, Rozanski GJ and Zucker IH (2017) Cardiac sympathetic afferent reflex control of cardiac function in normal and chronic heart failure states. *The Journal of physiology* **595**:2519-2534.

Watson CJ, Glezeva N, Horgan S, Gallagher J, Phelan D, McDonald K, Tolan M, Baugh J, Collier P and Ledwidge M (2020) Atrial Tissue Pro-Fibrotic M2 Macrophage Marker CD163+, Gene Expression of Procollagen and B-Type Natriuretic Peptide. *Journal of the American Heart Association* **9**:e013416.

Wiersma M, Meijering RAM, Qi XY, Zhang D, Liu T, Hoogstra-Berends F, Sibon OCM, Henning RH, Nattel S and Brundel B (2017) Endoplasmic Reticulum Stress Is Associated With Autophagy and Cardiomyocyte Remodeling in Experimental and Human Atrial Fibrillation. *Journal of the American Heart Association* **6**.

Wu Y, Hu Z, Wang D, Lv K and Hu N (2020) Resiniferatoxin reduces ventricular arrhythmias in heart failure via selectively blunting cardiac sympathetic afferent projection into spinal cord in rats. *European journal of pharmacology* **867**:172836.

Yuan Y, Zhao J, Gong Y, Wang D, Wang X, Yun F, Liu Z, Zhang S, Li W, Zhao X, Sun L, Sheng L, Pan Z and Li Y (2018) Autophagy exacerbates electrical remodeling in atrial fibrillation by ubiquitin-dependent degradation of L-type calcium channel. *Cell death & disease* **9**:873.

Zhang D, Wu CT, Qi X, Meijering RA, Hoogstra-Berends F, Tadevosyan A, Cubukcuoglu Deniz G, Durdu S, Akar AR, Sibon OC, Nattel S, Henning RH and Brundel BJ (2014) Activation of

histone deacetylase-6 induces contractile dysfunction through derailment of alpha-tubulin proteostasis in experimental and human atrial fibrillation. *Circulation* **129**:346-358.

Zhou X and Dudley SC, Jr. (2020) Evidence for Inflammation as a Driver of Atrial Fibrillation. *Frontiers in cardiovascular medicine* **7**:62.

Zhu H, Sun X, Wang D, Hu N and Zhang Y (2015) Doxycycline ameliorates aggregation of collagen and atrial natriuretic peptide in murine post-infarction heart. *European journal of pharmacology* **754**:66-72.

Zhu PJ, Khatiwada S, Cui Y, Reineke LC, Dooling SW, Kim JJ, Li W, Walter P and Costa-Mattioli M (2019) Activation of the ISR mediates the behavioral and neurophysiological abnormalities in Down syndrome. *Science* **366**:843-849.

Zyryanova AF, Weis F, Faille A, Alard AA, Crespillo-Casado A, Sekine Y, Harding HP, Allen F, Parts L, Fromont C, Fischer PM, Warren AJ and Ron D (2018) Binding of ISRIB reveals a regulatory site in the nucleotide exchange factor eIF2B. *Science* **359**:1533-1536.

Footnotes.

This work was supported by the National Natural Science Foundation of China [Grant 81670301].

JPET Fast Forward. Published on July 2, 2021 as DOI: 10.1124/jpet.121.000491
This article has not been copyedited and formatted. The final version may differ from this version.

Tables

Table 1 Echocardiographic data of experimental groups.

	Sham+vehicle (*n* = 11)	**Sham + ISRIB (*n* = 12)**	**MI +vehicle (*n* = 11)**	**MI + ISRIB (*n* = 12)**
LVIDd (cm)	0.615 ± 0.037	0.609 ± 0.044	0.716 ± 0.053	0.648 ± 0.052
LVIDs (cm)	0.290 ± 0.025	0.298 ± 0.028	0.478 ± 0.043*	0.336 ± 0.032$^{\#}$
LVPWd (cm)	0.199 ± 0.011	0.181 ± 0.012	0.185 ± 0.014	0.192 ± 0.015
EDV (ml)	0.523 ± 0.108	0.561 ± 0.118	0.848 ± 0.156	0.658 ± 0.122
ESV (ml)	0.435 ± 0.098	0.457 ± 0.108	0.581 ± 0.132	0.524 ± 0.144
EF (%)	87.138 ± 3.821	85.805 ± 4.11	48.659 ± 2.38**	67.326 ± 3.477$^{**\#\#}$
FS (%)	53.443 ± 2.867	52.672 ± 2.958	25.675 ± 2.308**	38.647 ± 2.903$^{*\#}$

LVIDd, left ventricular internal diameter at end-diastole; LVIDs, left ventricular internal diameter at end-systole; LVPWd, left ventricular posterior wall thickness at end-diastole; EDV, end-diastolic volume; ESV, end-systolic volume; LVPWs, left ventricular posterior wall thickness at end-systole; EF, ejection fraction; FS, fractional shortening. All data are shown as means ±s.e.m. Multiple groups were assessed using one-way analysis of variance (ANOVA) followed by the post-hoc Newman–Keuls multiple comparison test. $^{*}P < 0.05$, $^{**}P < 0.01$ vs. Sham group; $^{\#}P < 0.05$, $^{\#\#}P < 0.01$ vs. MI group.

Table 2. Characterization of the surface ECG

	Sham+vehicle (*n* = 11)	Sham + ISRIB (*n* = 12)	MI+vehicle (*n* = 11)	MI + ISRIB (*n* = 12)
Heart rate (bpm)	425.3 ± 6.9	418.6 ± 6.7	445.3 ± 7.8	438.6 ± 6.5
P (ms)	21.62 ± 0.67	23.45 ± 0.85	35.44 ± 0.78**	26.02 ± 0.92$^{**\#\#}$
PR (ms)	46.45 ± 1.23	48.38 ± 1.16	53.77 ± 1.82**	46.73 ± 1.32$^{\#\#}$
QRS (ms)	22.65 ± 0.43	23.65 ± 0.61	38.73 ± 0.68**	26.69 ± 0.71$^{**\#\#}$
QT (ms)	51.98 ± 1.89	54.42 ± 1.79	64.55 ± 1.18**	53.61 ± 1.57$^{\#\#}$

All data are shown as means ± s.e.m. Significant differences between means were determined using one-way ANOVA with the Bonferroni *post hoc* test for multiple comparisons. $^{*}P < 0.05$, $^{**}P < 0.01$ vs. Sham group; $^{\#}P < 0.05$, $^{\#\#}P < 0.01$ vs. MI group.

Figures and legends

Figure 1. Effects of ISRIB on AF inducibility and duration post-MI. A. Representative images of ECG (lead II) with sinus rhythm and AF by a burst of rapid pacing. B. Inducibility of AF. C. Durations of induced AF. Data are shown as means ± s.e.m. The Chi-square test was used to compare the inducibility of atrial fibrillation. The Mann-Whitney U test was used to test the difference of AF duration between the two MI groups. $^{*}P < 0.05$ vs. Sham group; $^{\#}P < 0.05$ vs. MI group.

Figure 2. Effects of ISRIB on the interstitial fibrosis of the left atria (LA) post-MI. A–C. Representative images of left atrial tissues at 7-day post-MI subjected to the Masson trichrome staining, alpha smooth muscle actin (α-SMA), or collagen I immunohistochemistry. D-F. Quantitative analysis of fibrosis, α-SMA, and type I collagen volume fraction. Data are shown as means ±s.e.m. Differences between means were determined by one-way ANOVA with the Bonferroni *post hoc* test for multiple comparisons $^{*}P < 0.05$, $^{**}P < 0.01$ vs. Sham group; $^{\#}P < 0.05$, $^{\#\#}P < 0.01$ vs. MI group.

Figure 3 Effects of ISRIB on the atrial expression of the eukaryotic initiation factor 2α (eIF2α) and the activating transcription factor 4 (ATF4) post-MI. A. Representative fluorescent immunostaining images of ATF4 in the left atria at seven days after MI (Scale bar = 50 μm). B. Quantitative assessment of ATF4-positive nuclei in the left atria. C. Representative Western blot images of total eIF2α, phosphorylated eIF2α (p-eIF2α), and ATF4 in

atria. D. Quantitative analysis of the expression of phosphorylated eIF2α relative to total eIF2α. E. Quantitative analysis of the expression of ATF4 relative to GAPDH. Data are shown as means ± s.e.m. Significant differences between means were determined by one-way ANOVA with the Bonferroni *post hoc* test for multiple comparisons. $^{*}P < 0.05$, $^{**}P < 0.01$ vs. Sham group; $^{\#}P < 0.05$, $^{\#\#}P < 0.01$ vs. MI group.

Figure 4 Effects of ISRIB on the atrial inflammation post-MI. A-B. Representative fluorescent immunostaining images of inflammatory cell infiltration in the left atria at seven days after MI (Scale bar = 50 μm). C-E. Quantitative assessment of CD68, iNOS, or CD163 and CD68-positive ($CD68^{+}$， $iNOS^{+}/CD68^{+}$, and $CD163^{+}/CD68^{+}$) area of cells. Data are shown as means ±s.e.m. Significant differences between means were determined by one-way ANOVA with the Bonferroni *post hoc* test for multiple comparisons. $^{*}P < 0.05$, $^{**}P < 0.01$ vs. Sham group; $^{\#}P < 0.05$, $^{\#\#}P < 0.01$ vs. MI group.

Figure 5 Effects of ISRIB on the atrial expression of autophagy-related protein post-MI. A. Representative fluorescent immunostaining images of autophagy-related protein LC3 (green) in the left atria at seven days after MI (Scale bar = 50 μm). B. Representative Western blot images of the autophagy-related protein LC3 in the left atria. C-D. Quantitative analysis of the expression of LC3-II relative to GAPDH and the ratio of LC3-II to LC3-I. Data are shown as means ±s.e.m. Significant differences between means were determined by one-way ANOVA with the Bonferroni *post hoc* test for multiple comparisons. $^{*}P < 0.05$, $^{**}P < 0.01$ vs. Sham group; $^{\#}P <$

0.05, ##P < 0.01 vs. MI group.

Figure 6 Effects of ISRIB on atrial expression of connexin43 (Cx43) post-MI. A. Representative fluorescent immunostaining images of Cx43 (green) in the left atria at 7 days after MI (Scale bar = 100 μm). B. Quantitative assessment of Cx43 expression in the left atria. Data are shown as means ±s.e.m. Significant differences between means were determined by one-way ANOVA with Bonferroni *post hoc* test for multiple comparisons. *P < 0.05, **P < 0.01 vs. Sham group; #P < 0.05, ##P < 0.01 vs. MI group.

Figure 7 Effects of ISRIB on atrial expression of the ion channel protein post-MI. A. Representative Western blot images of ion channel protein in the left atria at seven days after MI. B–D. Quantitative analysis of the expression levels of Nav1.5, Cav 1.2, and Kv4.3 relative to GAPDH. Data are shown as means ± s.e.m. Significant differences between means were determined by one-way ANOVA with Bonferroni *post hoc* test for multiple comparisons. *P<0.05, **P<0.01 vs. Sham group; #P <0.05, ##P<0.01 vs. MI group.

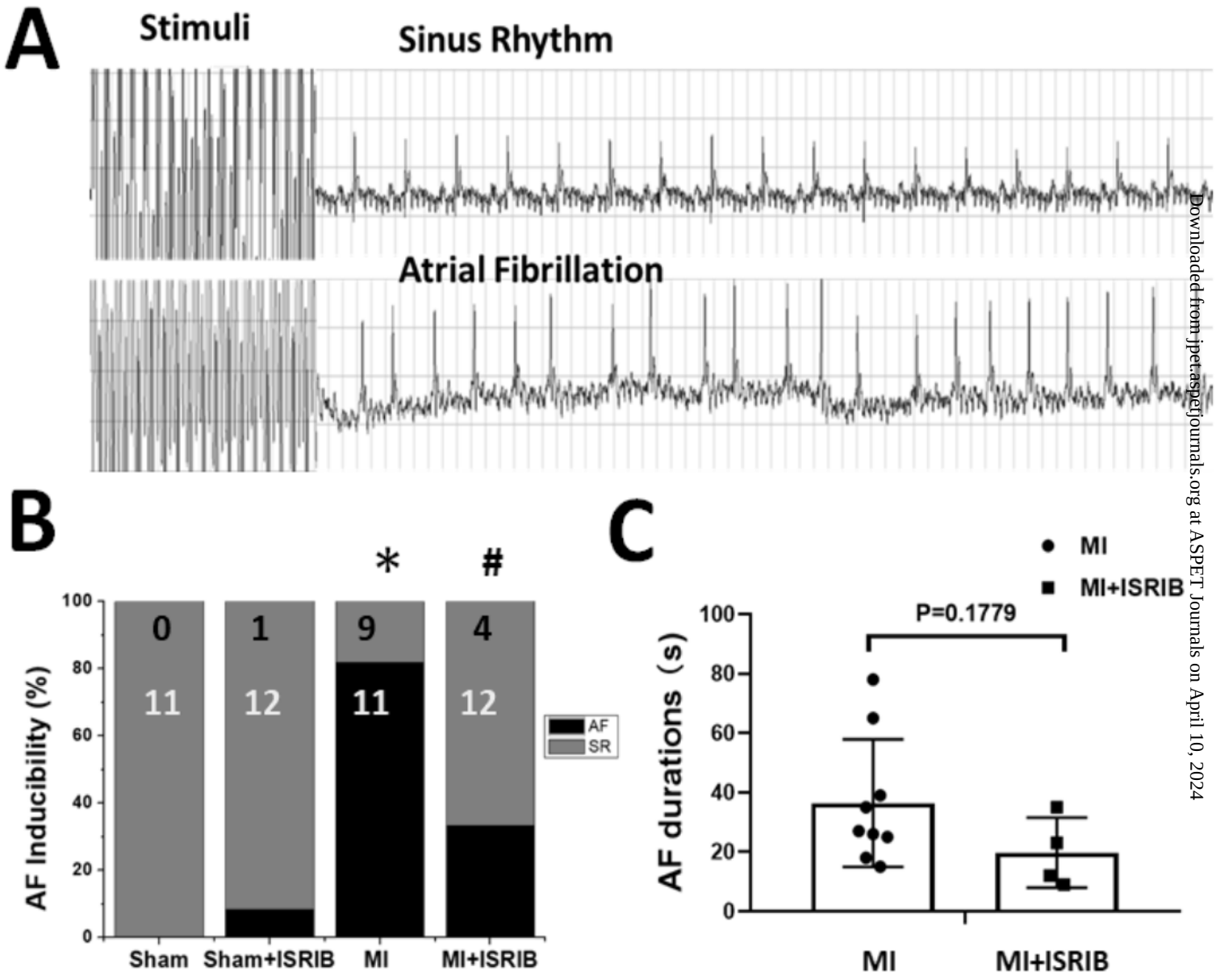

Figure 1

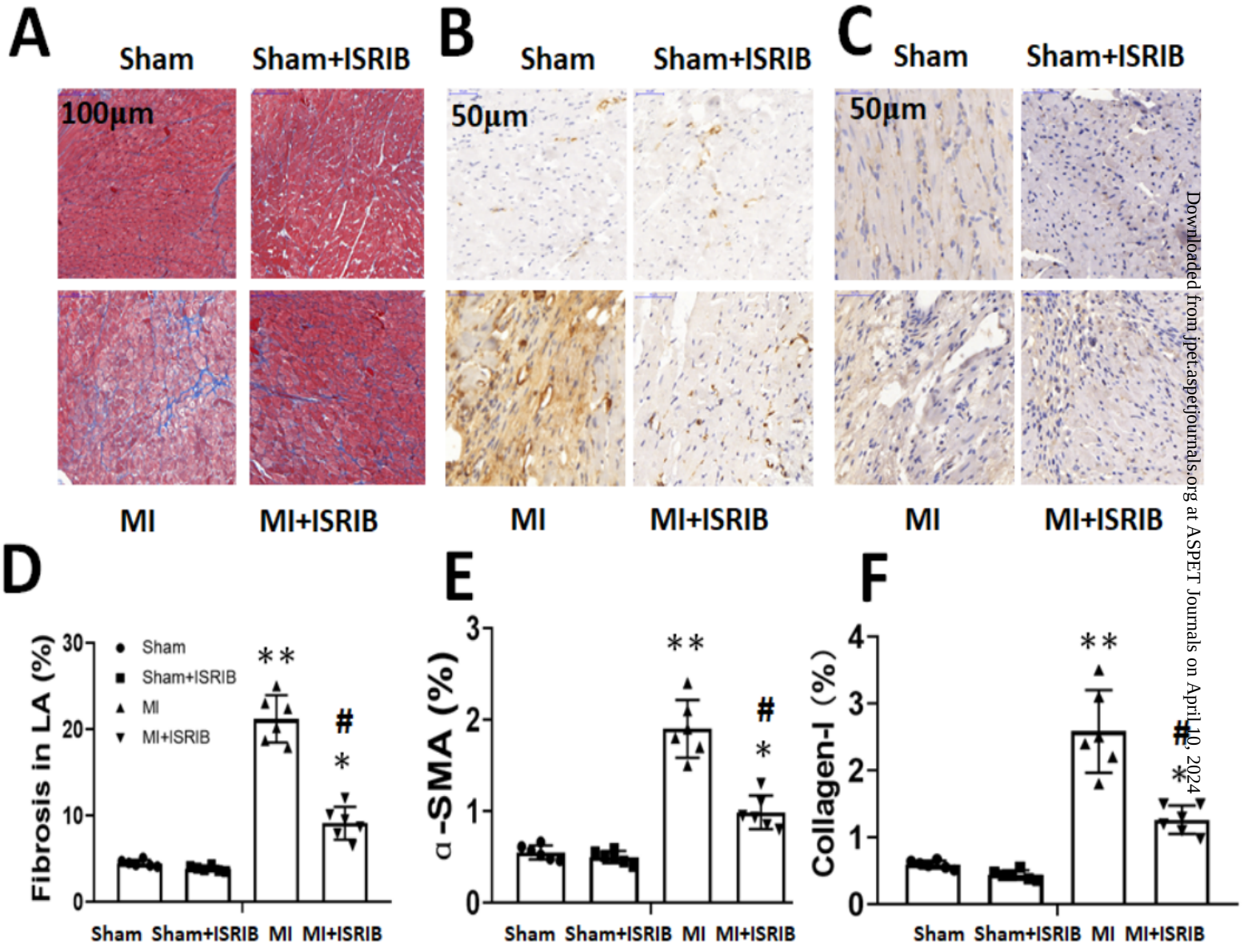

Figure 2

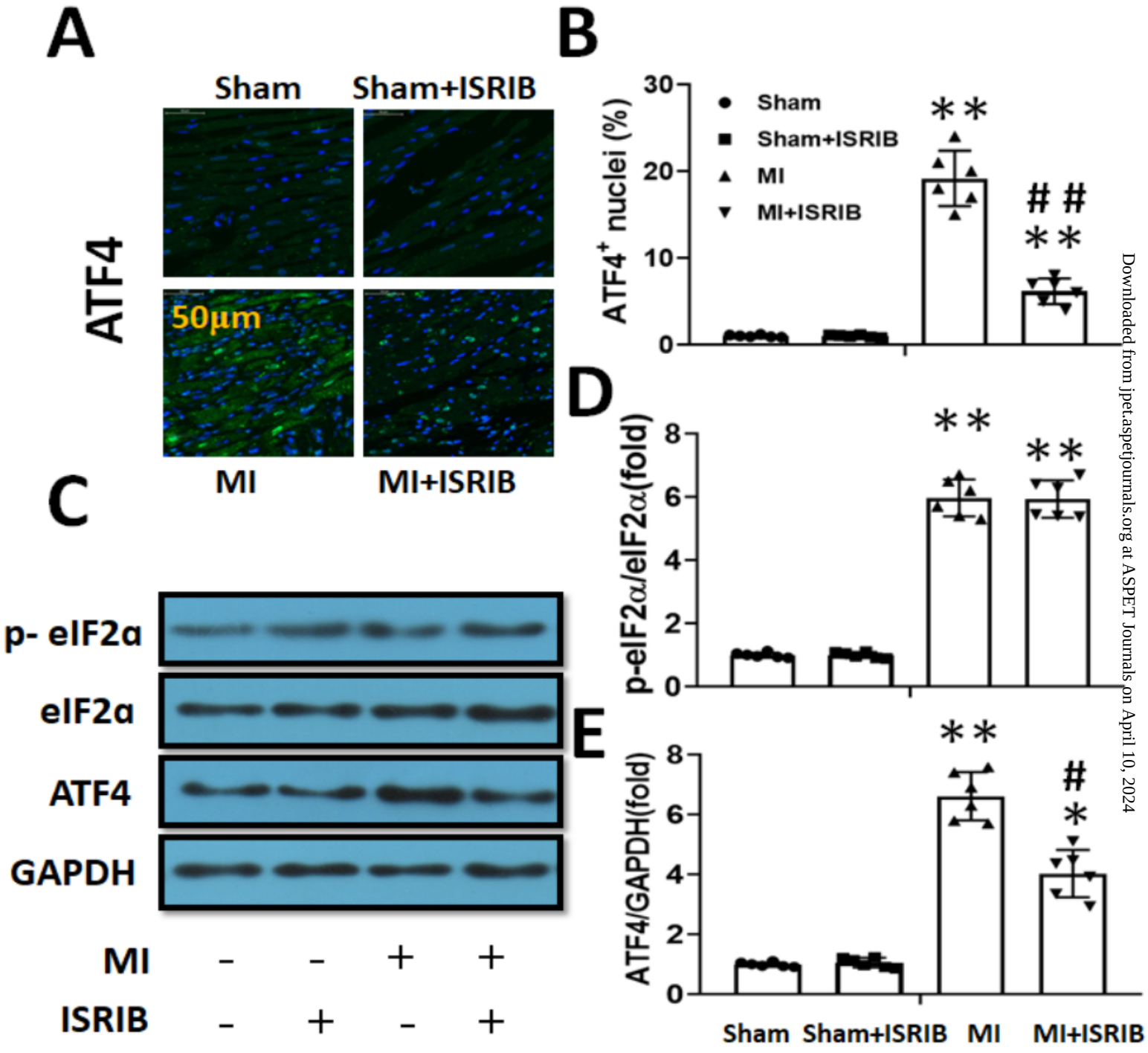

Figure 3

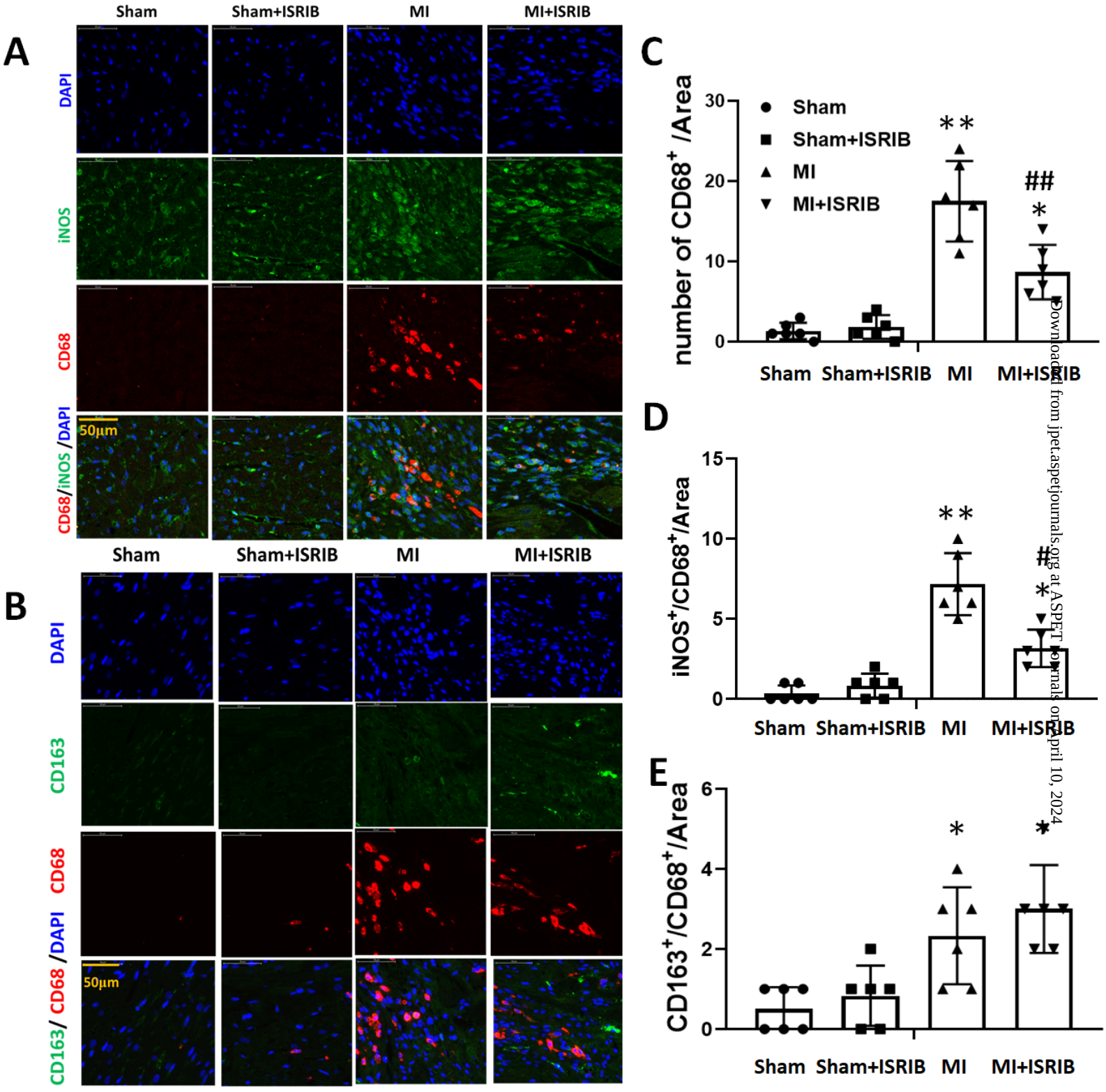

Figure 4

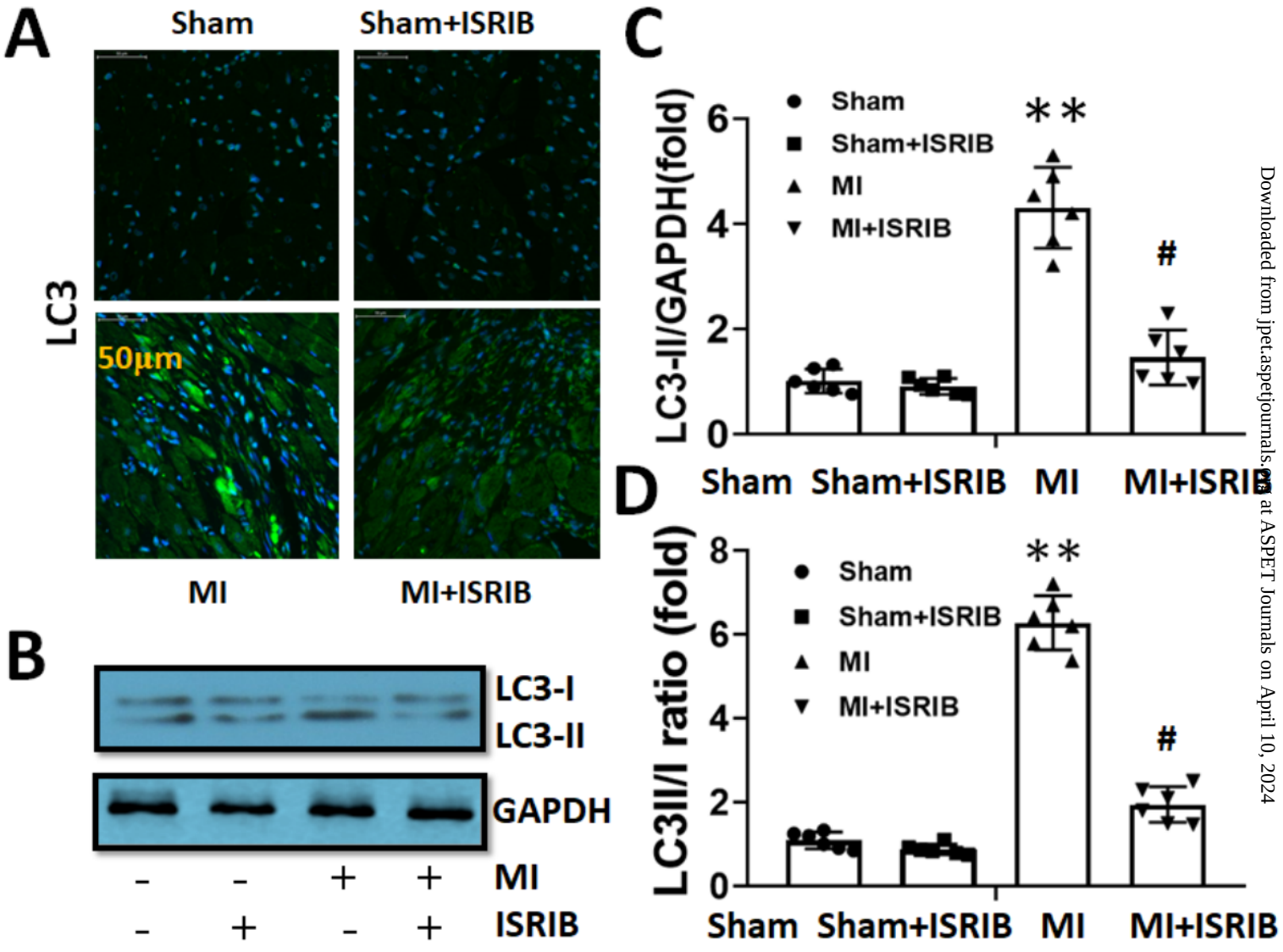

Figure 5

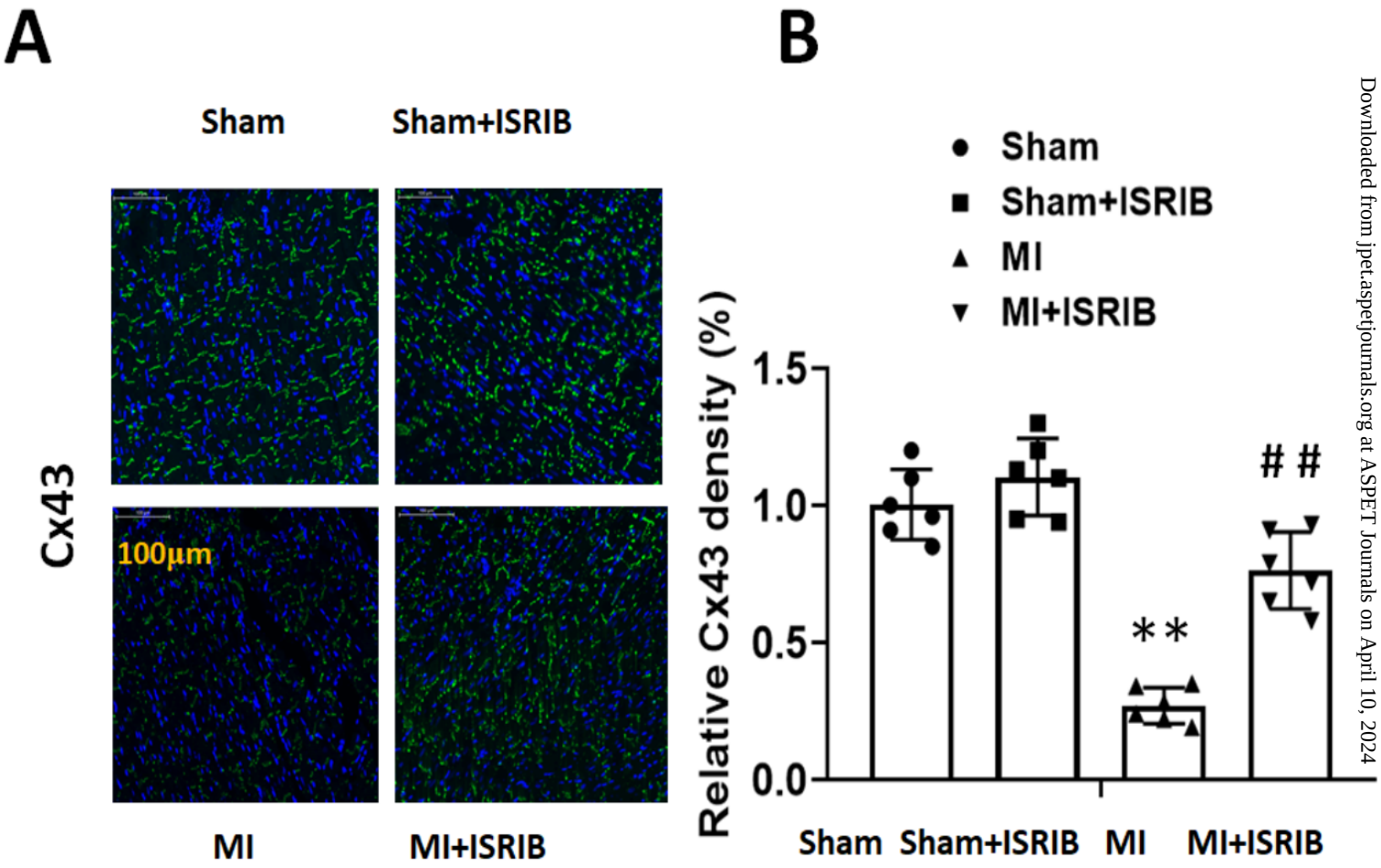

Figure 6

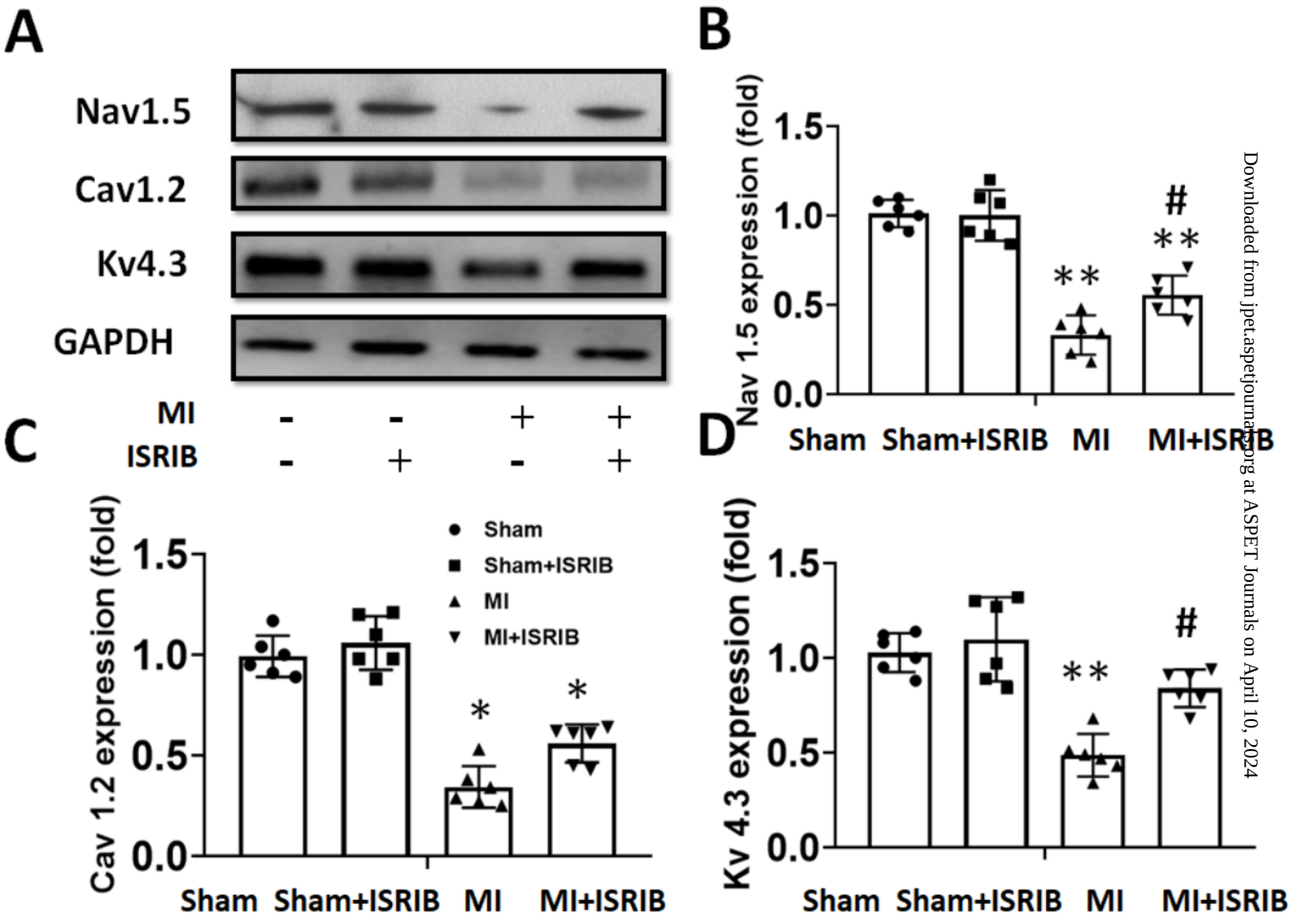

Figure 7

Supplemental Data

Small-molecule ISRIB reduces susceptibility to postinfarct atrial fibrillation in rats via the inhibition of integrated stress responses

Zhang T[1,2], Wu Y[1], Hu Z[1], Xing W[1,3], LV K[3], Hu N[1, 3, 4], Wang D[1,3*].

Dosage selection experimental

The dosage selection was based on previous reports with minor modifications (Barragán-Iglesias et al., 2019; Onat et al., 2019). In order to confirm the dosage of ISRIB, we referred to previous report about ISRIB tolerability (Briggs et al., 2017). In brief, a myocardial ischemia model of rats (n=12) with isoproterenol intraperitoneal injection (5mg/kg/d in 0.5ml saline) once daily for 10 days based on previous studies (Krenek et al., 2009; Gong et al., 2014). Animals were administered either vehicle or ISRIB (5 mg/kg and 0.25 mg/kg) once daily for 14 consecutive days (4 rate each group). Body weight and myocardial inflammation were evaluated at 14^{th} days.

Results

As shown in Supplementary Figure 3, ISO-induced myocardial ischemia caused a large amount of inflammatory cell infiltration mainly in the endocardium. CD68-positive macrophages increased significantly and were widely also distributed in the endocardium. High-dose ISRIB decreased CD68-positive macrophage infiltration. However, CD68-positive cells in the low-dose ISRIB group still maintained a high degree of infiltration. Quantitative analysis showed that low-dose ISRIB intervention continuously for 14 days did not significantly inhibit the infiltration of CD68-positive cells (Supplementary Figure 4B).

We also evaluate the weight gain of rats after two weeks ISRIB administration. As shown in Supplementary Figure 4A, rats in high-dose of ISRIB group have lower weight gain than vehicle or low-dose of ISRIB group.

References

Barragán-Iglesias P, Kuhn J, Vidal-Cantú GC, Salinas-Abarca AB, Granados-Soto V, Dussor GO, Campbell ZT and Price TJ (2019) Activation of the integrated stress response in nociceptors drives methylglyoxal-induced pain. *Pain* 160:160-171.

Briggs DI, Defensor E, Memar Ardestani P, Yi B, Halpain M, Seabrook G and Shamloo M (2017) Role of Endoplasmic Reticulum Stress in Learning and Memory Impairment and Alzheimer's Disease-Like Neuropathology in the PS19 and APP(Swe) Mouse Models of Tauopathy and Amyloidosis. *eNeuro* 4.

Gong W, Yan M, Chen J, Chaugai S, Chen C and Wang D (2014) Chronic inhibition of cyclic guanosine monophosphate-specific phosphodiesterase 5 prevented cardiac fibrosis through inhibition of transforming growth factor beta-induced Smad signaling. *Frontiers of medicine* 8:445-455.

Krenek P, Kmecova J, Kucerova D, Bajuszova Z, Musil P, Gazova A, Ochodnicky P, Klimas J and Kyselovic J (2009) Isoproterenol-induced heart failure in the rat is associated with nitric oxide-dependent functional alterations of cardiac function. *European journal of heart failure* 11:140-146.

Onat UI, Yildirim AD, Tufanli O, Cimen I, Kocaturk B, Veli Z, Hamid SM, Shimada K, Chen S, Sin J, Shah PK, Gottlieb RA, Arditi M and Erbay E (2019) Intercepting the Lipid-Induced Integrated Stress Response Reduces Atherosclerosis. *Journal of the American College of Cardiology* 73:1149-1169.

Tables and figures

Supplementary Table 1

Lists of Antibodies

Antibodies for IHC			
ATF4	Abcam ab23760	1:300	
LC3	Abcam ab48394	1:200	
a-SMA	Abcam ab7817	1:200	
Collagen-I	Abcam ab34710	1:200	
CD68	Abcam ab213363	1:400	
CD163	Abcam ab156769	1:400	
iNOS	Abcam ab49999	1:400	
Cx43	Abcam ab11369	1:400	
Antibodies for WB			
EIF2α	Cell Signaling CST#5324	1:1000	38
Phospho-eIF2α	Cell Signaling CST#3398	1:1000	38
ATF4	Abcam ab23760	1:2000	39
LC3	Abcam ab48394	1:2000	15，17
Nav1.5	Abcam ab86231	1:1000	168
Cav1.2	Abcam ab81980	1:1000	249
Kv4.3	Abcam ab ab228944	1:1000	73
GAPDH	Abcam ab8245	1:5000	37
Goat anti-Mouse IgG（H+L）	Thermo Pierce CST#：31160	1:5000	
Goat anti-Rabbit IgG（H+L）	Thermo Pierce CST#：31210	1:5000	

Supplementary Figure S1: Scheme of experimental design, group and mortality. MI, Myocardial infarction; UCG, Ultrasound Cardiogram; ECG, Electrocardiogram.

Supplementary Figure S2: Connex43 (Cx43) distribution in atrial tissues between MI and Sham groups. MI, Myocardial infarction.

Supplementary Figure 3: Representative fluorescent immunostaining images of CD68 positive cells in the inner layer of the heart 14^{th} days myocardial ischemia by isoproterenol intraperitoneal injection (Scale bar = 50 µm).

Supplementary Figure 4: A. Weight gain in different groups. High dose of ISRIB (5 mg/kg) have lower body weights compared to Vehicle and low dose of ISRIB (0.25 mg/kg). B. Quantitative assessment of CD68-positive ($CD68^{+}$) area of cells. Data are shown as mean ± s.e.m. (4 rat each groups). Differences between means were determined using the one-way ANOVA coupled with the Bonferroni post hoc test for multiple comparisons. A value of $P < 0.05$ was considered significant difference.

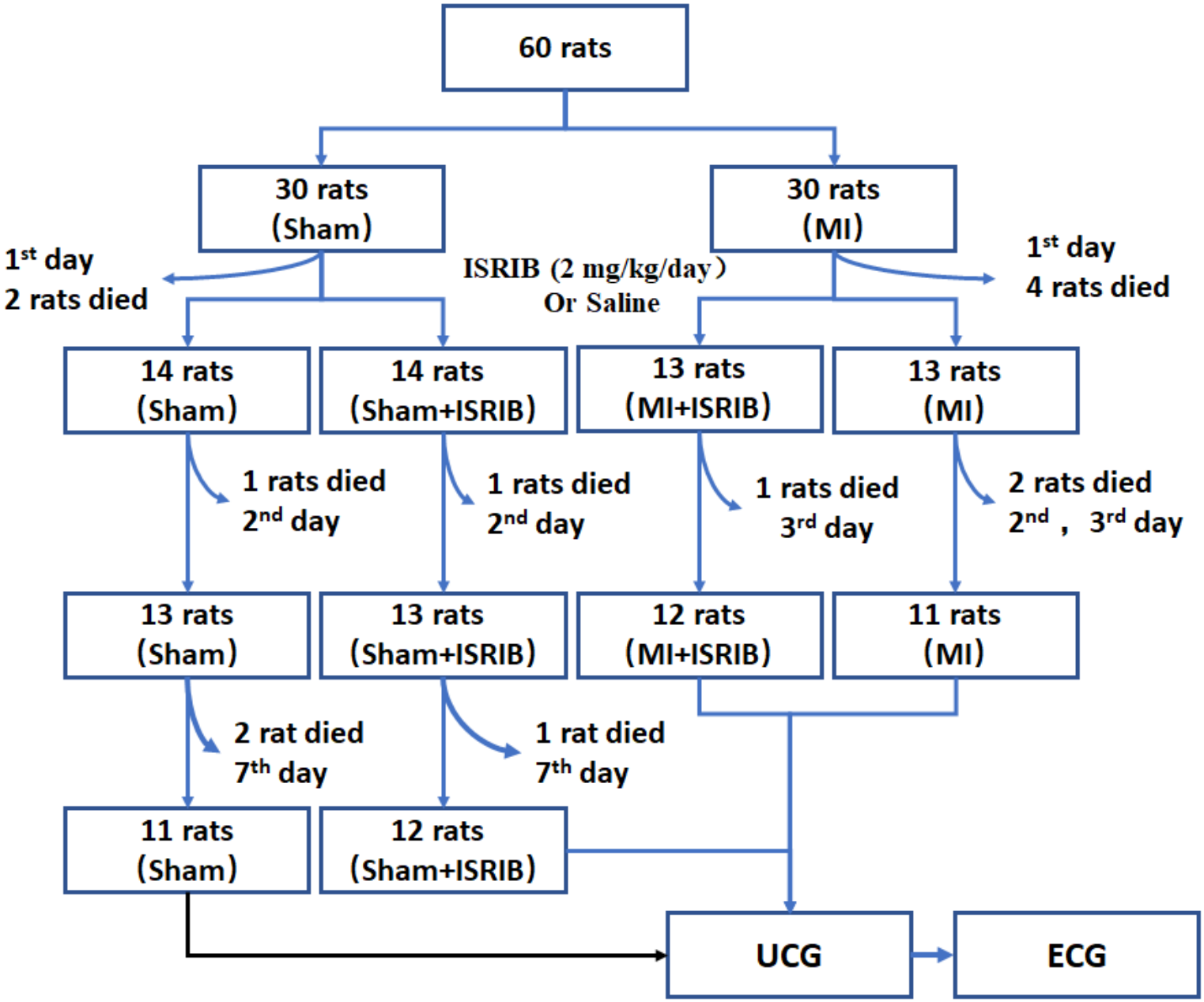

Supplementary figure 1

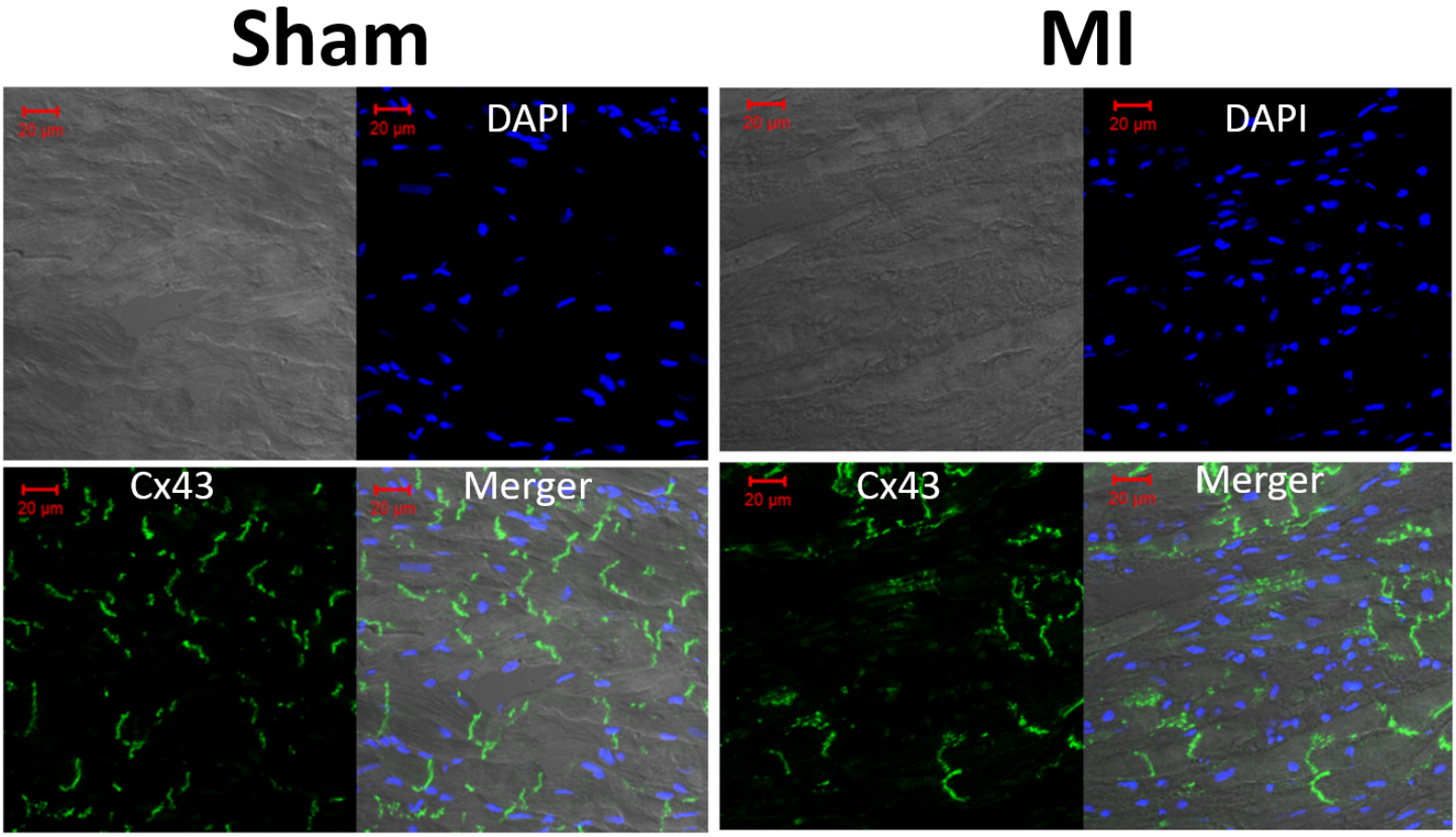

Supplementary figure 2

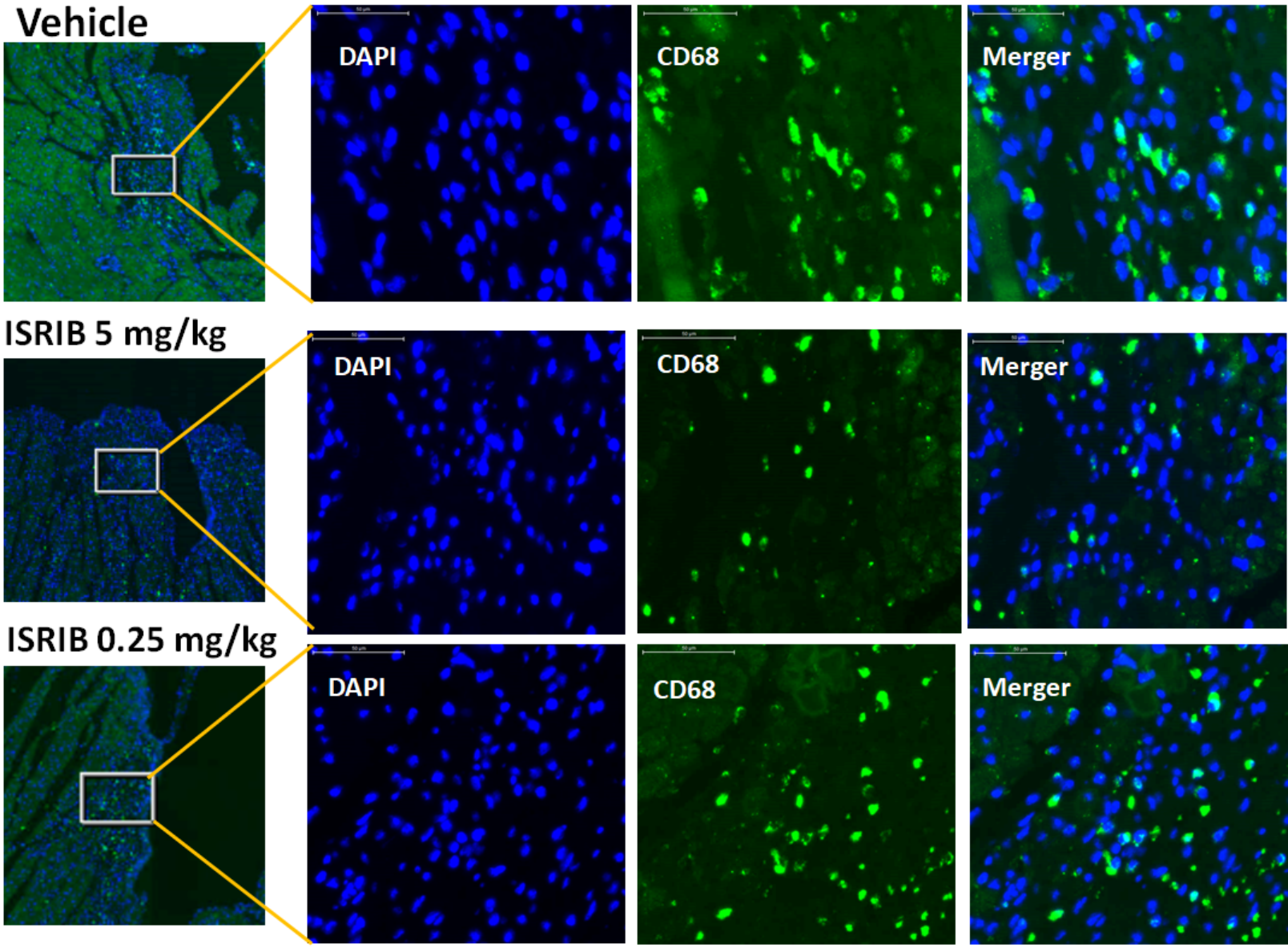

Supplementary figure 3

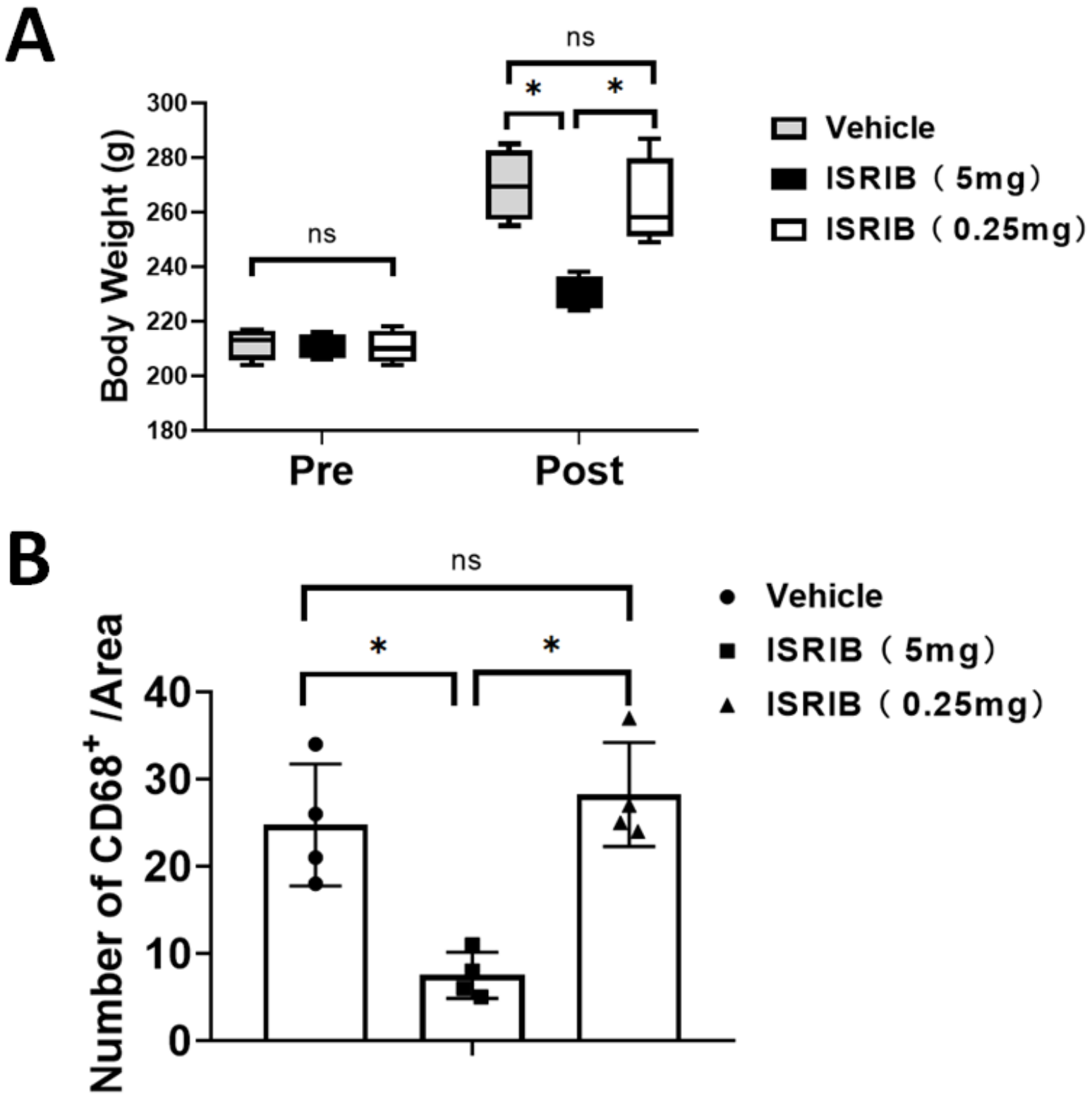

Supplementary figure 4